Knudson, W., Biswas, C., Li, X.-Q., Nemec, R. E., & Toole, B. P. (1989) in *The Biology of Hyaluronan* (Evered, D., & Whelan, J., Eds.) pp 150-169, Wiley, Chichester, U.K.
LeBoeuf, R. D., Raja, R. H., Fuller, G. M., & Weigel, P. H. (1986) *J. Biol. Chem. 261*, 12586-12592.
Lowry, O. H., Rosebrough, N. J., Farr, A. L., & Randall, R. J. (1951) *J. Biol. Chem. 193*, 265-275.
McGary, C. T., Raja, R. H., & Weigel, P. H. (1989) *Biochem. J. 257*, 875-884.
Oka, J. A., & Weigel, P. H. (1987) *J. Cell Physiol. 133*, 243-252.
Perides, G., Lane, W. S., Andrews, D., Dahl, D., & Bignami, A. (1989) *J. Biol. Chem. 264*, 5981-5987.
Raja, R. H., LeBoeuf, R. D., Stone, G. W., & Weigel, P. H. (1984) *Anal. Biochem. 139*, 168-177.
Raja, R. H., McGary, C. T., & Weigel, P. H. (1988) *J. Biol. Chem. 263*, 16661-16668.
Scott, J. E. (1960) *Methods Biochem. Anal. 8*, 145-197.
Smedsrod, B., Pertoft, H., Eriksson, S., Fraser, J. R. E., & Laurent, T. C. (1984) *Biochem. J. 223*, 617-626.
Smedsrod, B., Malmgren, M., Ericsson, J., & Laurent, T. C. (1988) *Cell Tissue Res. 235*, 39-45.
Smedsrod, B., Pertoft, H., Gustafson, S., & Laurent, T. C. (1990) *Biochem. J. 266*, 313-327.
Smith, C. E., Musich, P. R., & Johnson, D. A. (1989) *Anal. Biochem. 177*, 212-219.
Stamenkovic, I., Aruffo, A., Amiot, M., & Seed, B. (1991) *EMBO J. 10*, 343-348.
Toole, B. (1981) in *Cell Biology of the Extracellular Matrix* (Hay, E. D., Ed.) pp 259-294, Plenum Press, New York.
Turley, E. A. (1984) *Cancer Metastasis Rev. 3*, 325-339.
Turley, E. A., Brassel, P., & Moore, D. (1990) *Exp. Cell Res. 187*, 243-249.
Underhill, C. B., & Dorfman, A. (1978) *Exp. Cell Res. 117*, 155-164.
Underhill, C. B., & Toole, B. P. (1980) *J. Biol. Chem. 255*, 4544-4549.
Weigel, P. H., Fuller, G. M., & LeBoeuf, R. D. (1986) *J. Theor. Biol. 119*, 219-234.
Yannariello-Brown, J., & Weigel, P. H. (1991) *J. Cell Biol. 115*, 262 (Abstract).
Yannariello-Brown, J., Wewer, U., Liotta, L. A., & Madri, J. A. (1988) *J. Cell Biol. 106*, 1773-1786.
Yannariello-Brown, J., McGary C. T., & Weigel, P. H. (1992) *J. Cell. Biochem.* (in press).
Yoneda, M., Suzuki, S., & Kimata, K. (1990) *J. Biol. Chem. 265*, 5247-5257.

Hapten Conformation in the Combining Site of Antibodies That Bind Phenylphosphocholine†

Urs Bruderer,*,‡,§ David H. Peyton,*,∥ Elisar Barbar,∥ Jack H. Fellman,⊥ and Marvin B. Rittenberg‡
Department of Microbiology and Immunology, Oregon Health Sciences University, Portland, Oregon 97201, Department of Chemistry, Portland State University, Portland, Oregon 97207-0751, and Department of Biochemistry, Oregon Health Sciences University, Portland, Oregon 97201

Received August 26, 1991; Revised Manuscript Received October 7, 1991

ABSTRACT: We have shown previously that anti-phenylphosphocholine antibodies elicited by phosphocholine–keyhole limpet hemocyanin can be divided into two populations according to their ability to recognize the two hapten analogues *p*-nitrophenylphosphocholine (NPPC) and *p*-nitrophenyl 3,3-dimethylbutyl phosphate (NPDBP). These analogues differ from each other in that NPPC has a positively charged nitrogen in the choline moiety, whereas NPDBP lacks the positively charged nitrogen. Group II-A antibodies bind only NPPC, whereas group II-B antibodies bind both ligands. Here, by infrared and nuclear magnetic resonance spectroscopic investigations, we find that when free in solution NPPC has a predominantly fixed structure in which the termini approach each other, probably due to electrostatic interactions within the molecule; this "bent" structural feature is retained when the ligand is bound by antibody. In contrast, the structure of unbound NPDBP is less fixed, being characterized by rapidly interchanging conformations corresponding to an open chain structure with less overall proximity of the termini compared to NPPC. The overall shape of NPPC is essentially unaltered by binding, whereas in the case of NPDBP what was a minor conformation in the unbound state becomes the predominate conformation of the bound ligand. Thus, our results are consistent with these antibodies providing a molecular template for stabilizing the conformation of the bound ligand.

The majority of antibodies elicited by phosphocholine–keyhole limpet hemocyanin (PC–KLH)[1] belong to two populations which differ in their fine specificities. Group I antibodies react predominantly with the phosphocholine (PC) moiety, whereas group II antibodies require a phenyl group and have affinity for molecules such as *p*-nitrophenylphosphocholine (NPPC);

† This work was supported in part by a grant from the Oregon Affiliate of the American Heart Association to D.H.P. and NIH Grants AI14985 and AI26827 to M.B.R.
* Corresponding authors.
‡ Department of Microbiology and Immunology, Oregon Health Sciences University.
§ Present address: Department of Immunology, Swiss Serum and Vaccine Institute, CH-3001 Berne, Switzerland.
∥ Department of Chemistry, Portland State University.
⊥ Department of Biochemistry, Oregon Health Sciences University.

[1] Abbreviations: IR, infrared; NMR, nuclear magnetic resonance; NOE, nuclear Overhauser effect; NOESY, two-dimensional nuclear Overhauser effect spectroscopy; NPDBP, *p*-nitrophenyl 3,3-dimethylbutyl phosphate; NPPC, *p*-nitrophenylphosphocholine; PC–KLH, phosphocholine–keyhole limpet hemocyanin; TRNOE, transferred nuclear Overhauser effect.

0006-2960/92/0431-584$03.00/0

Table I: Binding Phenotypes of Anti-PC–KLH Antibodies (I_{50})[a]

antibody group[b]	inhibitor		
	PC	NPPC	NPDBP
group I	0.002–0.13[a]	0.01–0.27	4.6–>10
group II-A	>10	0.026–6.6	>10
group II-B	>10	0.06–0.8	0.28–6.5

[a] I_{50} values are defined as the inhibitor concentration (mM) required to inhibit 50% of antibody binding to PC–histone conjugates in an enzyme-linked immunosorbent assay (Chang et al., 1982). [b] Subsets of antibodies are as previously described (Bruderer et al. 1989).

NPPC closely mimics the antigenic group in PC–KLH (Chang et al., 1982). Recently (Bruderer et al., 1989), we showed that group II antibodies can be further subdivided according to their ability to recognize the NPPC analogue *p*-nitrophenyl 3,3-dimethylbutyl phosphate (NPDBP). This molecule differs from the zwitterion NPPC by lacking the positive charge in the choline moiety. Group II-A antibodies recognize NPPC but exhibit no significant binding to NPDBP. In contrast, group II-B antibodies can bind to either ligand. This is demonstrated by the I_{50} values summarized in Table I.

Here, utilizing infrared (IR) and nuclear magnetic resonance (NMR) spectroscopic analyses, we describe experiments designed to improve the understanding of the spatial interactions resulting in specific recognition of NPPC and NPDBP by monoclonal antibodies. Our results suggest that in solution NPPC and NPDBP differ in their conformational behaviors. NPPC can be described as a choline moiety similar to that of PC itself (Akutsu & Kyogoku, 1977; Pullman, et al., 1975; Richard et al., 1974). Here we show that the ends of the NPPC molecule are held near each other, whereas NPDBP is characterized by rapidly interchanging conformations, with less overall proximity of the termini. However, the antibody-bound conformation of each analogue is similar in that the termini of the ligand are held in close proximity to one another.

Materials and Methods

PC and NPPC were obtained from Sigma (St. Louis, MO), and NPDBP was synthesized as described (Bruderer et al., 1989). IR spectra were obtained using a Perkin Elmer 1800 FT-IR instrument, analyzing tablets containing 1 mg of sample/100 of KBr as described by Price (1972). Samples for NMR spectroscopy were dissolved directly into phosphate-buffered saline in ^2H_2O, and pH values were adjusted with Na^2OH or ^2HCl as needed. pH readings were not corrected for the isotope effect.

The production, antigen-binding characteristics, and nucleotide and deduced amino acid sequences of PCG1-2 ($\gamma1,\kappa$), PCG2b-3 ($\gamma2b,\lambda$), and PCG1-9 ($\gamma1,\lambda$) were described previously (Stenzel-Poore & Rittenberg, 1989). F_{ab} fragments were prepared from PCG1-9 using an Immunopure-Fab Kit according to the manufacturer's instructions (Pierce Chemicals, Rockford, IL). The final F_{ab} fragment was identified by HPLC and purified by affinity chromatography using PC–Sepharose and elution with NPPC followed by extensive dialysis as described previously (Chang et al., 1982).

Molecular conformation calculations were performed using an augmented MM2 force field (Allinger, 1977) with Tektronix CAChe molecular modeling hardware. Structures were calculated from a variety of starting geometries, with final geometries retained after convergence to $<10^{-3}$ kcal/mol.

NMR spectra were collected using a Bruker AMX-400 NMR spectrometer, at 400.14 MHz for ^1H and 161.98 MHz for ^{31}P. Samples were contained in 5-mm o.d. sample tubes, and the temperature was maintained at 37 °C. Spectra were collected with a repetition time of at least 5 s, employing quadrature. Chemical shifts were referenced to DSS (2,2-dimethyl-2-silapentane-5-sulfonate) through the residual water signal. One-dimensional NOE difference experiments were performed using a preirradiation time of 2 or 4 s in the sequence $[-\tau_{wt}-\tau_{irrad}-(\pi/2)_{obs}-\text{FID}-]_n$ or the inversion–recovery sequence $[-\tau_{wt}-(\pi)_{select}-\tau-(\pi/2)_{obs}-\text{FID}-]_n$. At least 128 scans were accumulated for each irradiation frequency, by cycling through the decoupling list after each 16 or 32 scans, and 5-Hz line-broadening factor was applied before Fourier transformation.

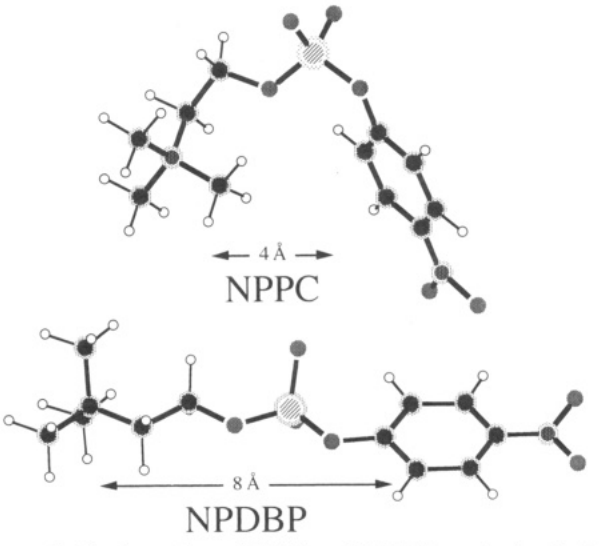

FIGURE 1: Conformations of NPPC and NPDBP as calculated using the MM2 parameters; bent for NPPC; extended for NPDBP.

Two-dimensional phase-sensitive ^1H NMR NOESY spectra (Kumar et al., 1980) were obtained with TPPI to obtain quadrature detection in t_1 (Marion & Wüthrich, 1983). A total of 320 t_1 values were used, and free induction decays in t_2 were recorded in 2048-point blocks, summing 32 acquisitions each. Solvent suppression, to avoid overfilling the 16-bit ADC, was achieved by saturation during the relaxation delay. The data sets were zero-filled to 512 × 2048 data point sets after apodization with a 30°-phase-shifted sine-bell-squared function. All spectra were processed on the spectrometer X-32 computer using the manufacturer's software, UXNMR.

Results

The relative proximity of the positive and negative charges in NPPC suggests that there may be an electrostatic interaction leading to restriction of molecular mobility. This is based on earlier studies on PC (Akutsu & Kyogoku, 1977; Richard et al., 1974). A calculation according to the MM2 protocol was performed to obtain the energetics for both a bent and an extended structure for NPPC and NPDBP (Figure 1); although we show a "bent" structure for NPPC and a fully extended structure for NPDBP, we performed calculations on both geometries for both molecules in the absence of solvent in order to obtain first approximations of the structures. Note that the distance between the aromatic ring and the trimethylammonium end of the molecule in the extended conformation is about twice that of the bent conformation. The bent structure for NPPC is calculated to be ~0.5 kcal/mol lower in energy than the fully extended structure, while the extended and bent conformations for NPDBP are nearly equal in energy. The calculations of Pullman et al. (1975) indicate that the PC molecule has a similar conformation to the PC portion of NPPC shown in Figure 1, in that the $C^\beta H_2$–$C^\alpha H_2$

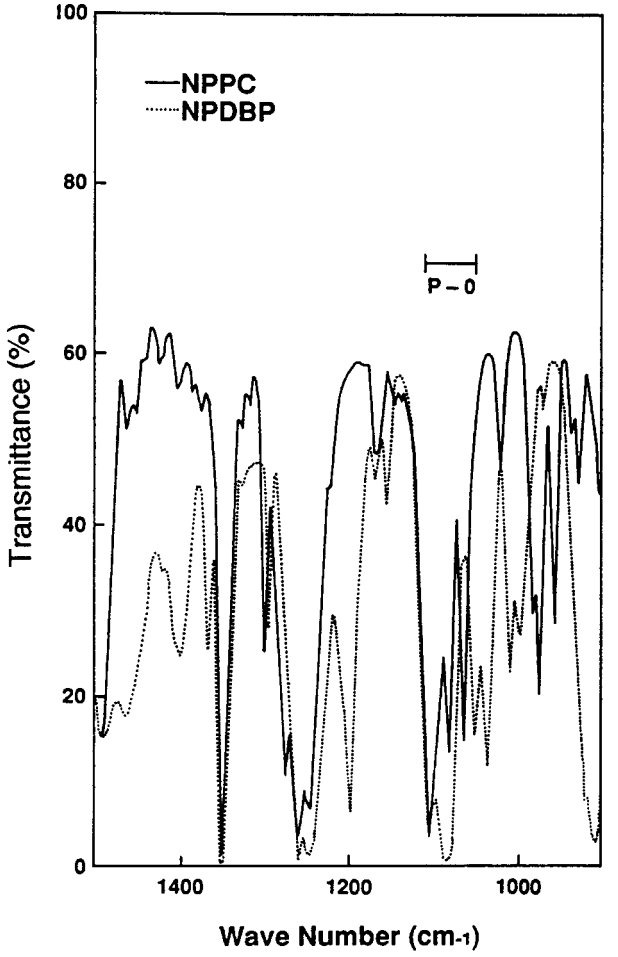

FIGURE 2: IR spectra for NPPC and NPDBP. These spectra were obtained using dry KBr pellets containing 1 mg of sample/100 mg of KBr.

bond is gauche; this bond angle was found not to be dependent on water solvation.

We recorded the IR spectra of NPPC and NPDBP; these are shown in Figure 2. In the P=O stretching region, there are bands at 1104 and 1094 cm^{-1} which are shifted toward higher energy for NPPC relative to NPDBP. This spectral shift indicates that the negatively charged phosphate moiety is interacting with the choline trimethylammonium. Nevertheless, these data are for the solid state and so may also be indicative of crystal packing and/or dimerization of the molecules.

In order to gain further information about the molecular conformations, NPPC and NPDBP were submitted to solution-state ^1H NMR analyses. Figure 3A,C,E demonstrates the appearance of the ^1H NMR spectra of PC, NPPC, and NPDBP; the resonance assignments provided are consistent with previous work on PC (Akutsu & Kyogoku, 1977; Richard et al., 1974) and are based on chemical shift and coupling constants. NPDBP (Figure 3E) exhibits a first-order spectrum in the upfield region, including coupling arising from the ^{31}P. The ^{31}P signal appears as a triplet with $J \sim 7$ Hz (not shown). Thus the ^{31}P–O–$C^{\alpha}H_2$–$C^{\beta}H_2$ spin system corresponds well to an open chain system, in which there is sufficient internal mobility to render the methylene protons equivalent within each pair. In contrast, the upfield region of the NPPC spectrum (Figure 3C) exhibits a complex set of overlapping multiplets for each methylene pair, precluding averaging of the methylene protons of NPPC by conformational mobility, at least on a time scale on the order of the NPPC coupling constants; this indicates that NPPC has a restricted conformational mobility. The ^{31}P NMR spectrum of NPPC supports this interpretation because it has the appearance of a distorted triplet (not shown). The ^1H NMR spectrum of PC was analyzed in detail by others (Akutsu & Kyogoku, 1977; Richard et al., 1974) and is similar to that of NPPC (Figure 3C). Thus, NPDBP, compared to NPPC or PC, is relatively unrestricted in the internal conformational mobility between its conformers.

The nuclear Overhauser effect (NOE) can provide estimates for average internuclear distances (Ernst et al., 1987). Figure 3B,D,F shows difference spectra resulting from irradiating the nine-proton singlet peak δ of each analogue. Positive NOEs are observed from each δ-$(CH_3)_3$ group to both methylene groups ($C^{\alpha}H_2$, $C^{\beta}H_2$); these proton sets have averaged positions not more than about 0.4–0.5 nm from the δ-$(CH_3)_3$ group. A positive NOE (~0.3%) is observed between the ortho-aromatic and the δ-protons [$-N(CH_3)_3^+$] of NPPC. The presence of this NOE combined with the fact that NPPC is conformationally restricted indicates that the major fraction of NPPC must exist in a conformation which places the two ends of the molecule near each other. NPDBP has an NOE (~0.2%) which is ~30% less than the NOE of NPPC from the δ-protons to the ortho-aromatic protons. Since NPDBP has a large degree of internal mobility, this NOE presumably arises from a minor fraction of the molecules which have their termini near each other. Neither the appearance of the spectra of NPPC and NPDBP nor these NOEs change over a large concentration range (1–100 mM), indicating that these results do not arise through molecular association. Without the electrostatic effects from the positively charged nitrogen, there seems to be less incentive for the two ends of NPDBP, on the time average, to approach each other and to maintain this conformation to the degree that occurs in NPPC.

In order to assess ligand conformations and internuclear distances when bound to antibody, we analyzed the transferred nuclear Overhauser effect (TRNOE) as described by others (Clore & Gronenborn, 1982; Glaudemans et al., 1990). Figure 4A shows the NMR spectrum of 100-fold excess of NPPC in the presence of the group II-A antibody PCG1-2. The line width of the nine-proton singlet [$-N(CH_3)_3^+$] of NPPC is broadened relative to that in Figure 3C; this broadening is much larger at lower ratios of hapten to antibody (e.g., 1:30, not shown). Under no conditions were two sets of NPPC resonances observed, demonstrating that the hapten is exchanging between free and bound forms in the "fast exchange" regime, indicating that a TRNOE analysis should be possible. Figure 4B is a representative two-dimensional NMR (NOESY) spectrum for this NPPC/PCG1-2 system, with a mixing time of 300 ms, and Figure 5 presents the set of NOE-buildup curves for TRNOE cross peaks between the meta-, α-, β-, and δ-proton sets and the ortho-phenyl protons. The bound $\rightleftarrows$ free exchange is sufficient to produce the observed negative TRNOEs. The observation that these TRNOE-buildup curves can be extrapolated to zero intensity at zero time is consistent with a primary NOE between each of the proton sets (Koide et al., 1989), although the observed TRNOEs may still also have a spin-diffusion component. In the absence of an accurate measurement of the off-rate for the complex (Glaudemans et al., 1990) or a complete relaxation matrix (Keepers & James, 1984), it is possible to use the initial buildup rate for the TRNOE to place a lower bound on internuclear distances (Clore & Gronenborn, 1982); this depends on the cross-relaxation rate (σ_{ij}) for proton sets i,j, and σ_{ij} is proportional to $1/(r_{ij})^6$. We estimate the meta- to ortho-proton TRNOE to build ~10–20-fold faster than the TRNOE between the

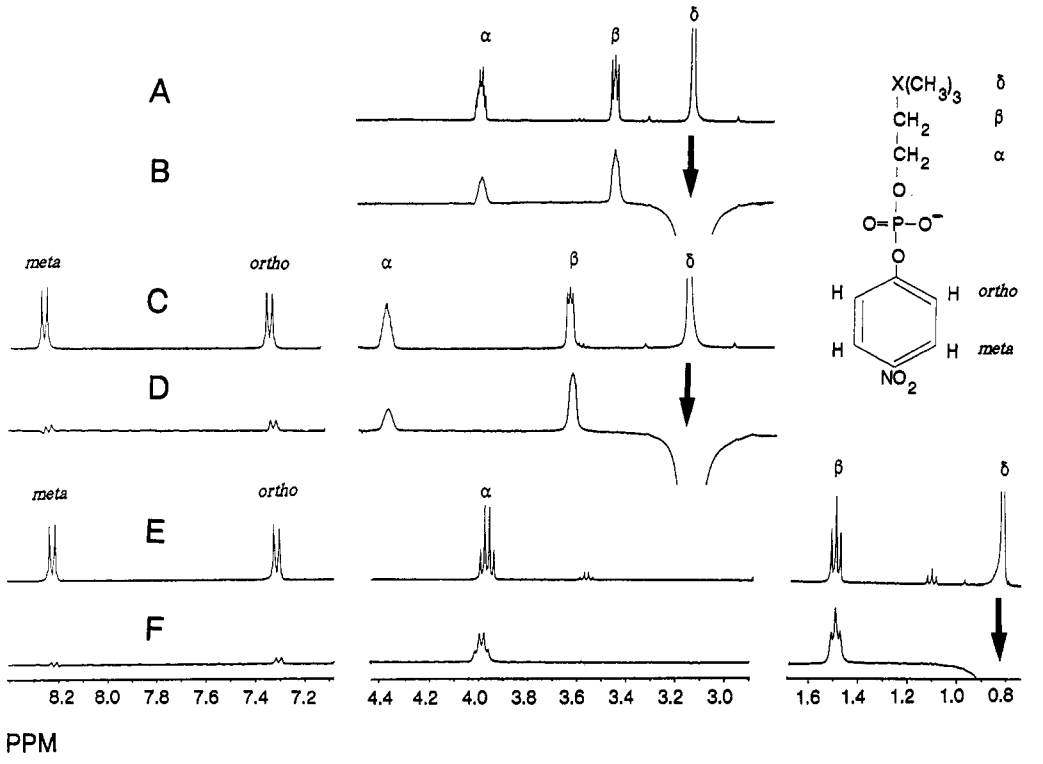

FIGURE 3: ^{1}H NMR spectroscopy of PC, NPPC, and NPDBP at 37 °C and pH 7.0. (A) PC. Note that this spectrum has very complex unresolved multiplets for the α- and β-CH_2's. (B) NOE difference spectrum for PC resulting from irradiating at peak δ. (C) NPPC. Note that this spectrum has complex unresolved multiplets for the α- and B-CH_2's. (D) NOE difference spectrum for NPPC resulting from irradiating at peak δ. Note the 0.3% NOE to the ortho-protons. (E) NPDBP. Note that this spectrum has clean multiplets for the α- and β-CH_2's. (F) NOE difference spectrum resulting from irradiating at peak δ. Note the 0.2% NOE to the ortho-protons. Each of the spectra were processed with a line-broadening factor of 0.3 Hz (A, C, and E) or 4 Hz (B, D, and F). The structure demonstrates the structures of NPPC (X = N^+) and NPDBP (X = C); PC (X = N^+) lacks the nitrophenyl moiety.

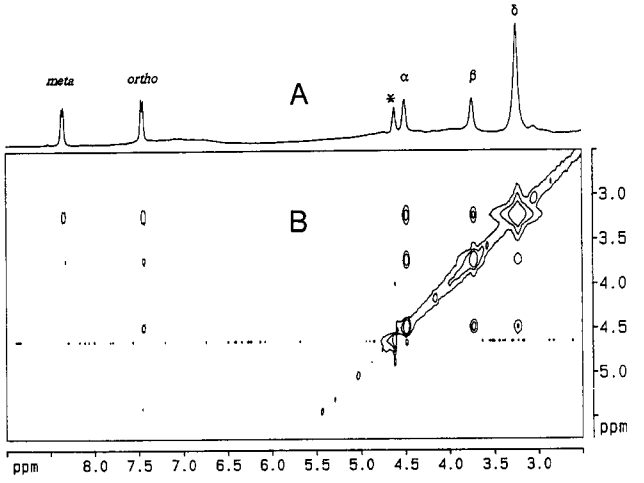

FIGURE 4: Two-dimensional TRNOE (NOESY) ^{1}H NMR spectrum for NPPC in the presence of PCG1-2 at 37 °C and pH 7.0. (A) Reference spectrum. Note that resonance δ is significantly broadened relative to NPPC alone (Figure 1C). (B) NOESY spectrum with a 300-ms mixing time. Note that cross peaks can be seen between peak δ and each of the other NPPC resonances.

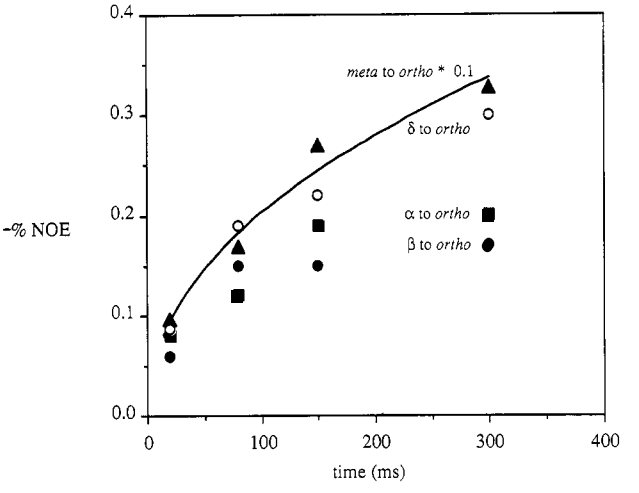

FIGURE 5: TRNOE buildup for NPPC in the presence of PCG1-2 at 37 °C and pH 7.0. The meta to ortho TRNOE data were multipled by 0.1 in order to fit the data on the same plot as the other TRNOEs. The meta to ortho TRNOE data are also fit to a logarithmic function. Note that each of the NOEs has an intercept at time ~0 ms and so has at least a primary NOE component.

ortho- and δ-protons. On the basis of the ortho- to meta-proton internuclear distance of 0.25 nm, the ortho to δ time-averaged distance calculates to be about 0.4 nm, the distance at which one expects a weak NOE.

Group II-B antibodies interact strongly with NPPC and NPDBP (Table I). We therefore examined NPDBP and NPPC, by TRNOEs, when bound to the group II-B antibody PCG2b-3. Results similar to those obtained for NPPC interacting with PCG1-2 were obtained with PCG2b-3 interacting with either NPPC or NPDBP, except that both negative and positive intramolecular hapten TRNOEs are observed. The positive TRNOEs are of lower magnitude than in the free hapten. The TRNOE between the δ-proton set and the aromatic ortho-protons is negative, so the bound hapten must be in a conformation which has its ends within 0.5 nm of each other when bound to PCG2b-3. However, the bound $\rightleftarrows$ free exchange seems to be significantly slower than in the NPPC/PCG1-2 (group II-A antibody) case described above, which could suggest that spin diffusion contributes significantly to these results.

In order to address the possible contribution of spin diffusion, we analyzed the interaction of NPDBP with the F_{ab}

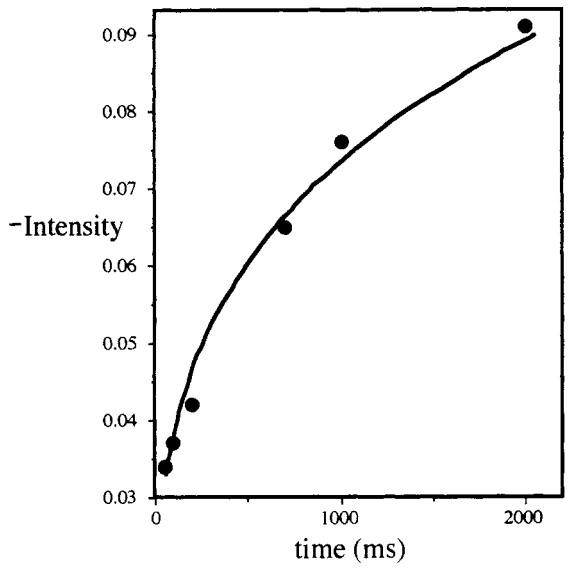

FIGURE 6: TRNOE buildup for NPDBP in the presence of PCG1-9 F_{ab} fragments at 37 °C and pH 7.0. The data, in arbitrary intensity units, are fit to a logarithmic function. Note that the TRNOE has an intercept at time ~0 ms and so has at least a primary NOE component.

fragment of group II-B antibody PCG1-9. Because of the F_{ab}'s lower molecular weight, its contribution to the negative TRNOE of the hapten is diminished as compared with NPDBP bound to the intact antibody (not shown). Therefore, only a set of 1-D NOE data is reported (Figure 6), to show the TRNOE-buildup curve resulting from inverting the singlet from $-C(CH_3)_3$ and observing the intensity of perturbation to the ortho-phenyl NMR signal. As in each of the previous cases, there is a primary TRNOE between the δ- and ortho-protons, demonstrating that the bound NPDBP time-averaged geometry must have its δ-proton "tail" within dipolar contact distance (<0.5 nm) of the phenyl ortho-protons. Even if exchange were quite slow, and spin diffusion a strong contributor to the observed TRNOEs at longer mixing times, the presence of a negative TRNOE at the shortest mixing time (20 ms) for this ~50-kDa system demonstrates that a major part of the observed TRNOE is primary and not a result of spin diffusion. Thus, the conformation of NPDBP, when bound to the PCG1-9 F_{ab} fragment, resembles that of NPPC or NPDBP when bound to PCG2b-3 or to intact PCG1-9.

Discussion

Our goal is to elucidate the structural basis of selectivity among antibodies generated in the antihapten response to PC–protein conjugates. Previously, we have shown that monoclonal antibodies can be classified according to their abilities to recognize the two PC analogues NPPC and NPDBP, which differ from one another in that the latter is lacking the positive charge (Bruderer et al., 1982). This difference implies that intramolecular ionic interactions might be a discriminating factor. Here, we show that NPPC and NPDBP differ in their conformational behaviors in the unbound state, but not in the bound state. The use of TRNOEs for evaluating bound ligand conformations in ligand–antibody and ligand–antibody fragment complexes is now well-established (Glaudemans et al., 1990; Anglister & Zilber, 1990; Zilber et al., 1990). Small, flexible molecules can be profitably studied in the bound state using TRNOEs (Bejling et al., 1988). Secondary ligand-binding sites can interfere in TRNOE data, especially when working with a large excess of ligand. In the experiments described here, however, we believe that the measurements for bound NPPC and NPDBP structures likely reflect binding to the primary site because other, group II-A, antibodies from the immune response to PC–KLH do not give significant TRNOEs with NPDBP (unpublished observations). If secondary binding sites were contributing in this system, we would have expected them to appear even in the absence of active site binding.

In contrast to the conformations found in the unbound state, NPDBP bound by antibodies appears to have a geometry similar to that of NPPC, suggesting that a similar steric fit of the two ligands is required (group II-A and group II-B antibodies) but not necessarily sufficient (group II-A antibodies). Group II-A antibodies may fail to bind NPDBP because either essential intermolecular ionic attraction is lacking or intramolecular ionic forces determining its spatial shape are missing or a combination of both. The broadening of the nine-proton resonance from the $-(CH_3)_3^+$ group of NPPC, when interacting with PCG1-2 (compare Figures 3C and 5A), suggests that electrostatic interactions may be involved which resemble those proposed from the classic crystallographic structure of the complex of PC–McPC603 (Satow et al., 1986; Segal et al., 1974).

Our results are consistent with two models, either the correct bent conformation of NPDBP interacts only with group II-B antibodies or these antibodies can initially bind a variety of conformers of NPDBP, which would subsequently attain their final bent conformation in the antibody-binding site. The bent structure for NPPC is calculated to be ~0.5 kcal/mol lower in energy than the hypothetical fully extended structure of NPPC, while the extended and bent conformations for NPDBP are similar in energy. Since unbound NPDBP is an equilibrium of rapidly interchanging conformations, including some with the termini in proximity, binding may occur by selecting bent molecules from the mixture. This notion is supported by the relatively small penalty in binding constant of group II-B antibodies binding NPDBP rather than NPPC, a factor of ~5 (Bruderer et al., 1989). In either event, the antibodies can be considered to be a molecular template for regulating the final stable ligand conformation. A similar result has recently been reported for a complex between a carbohydrate ligand and the monoclonal antibody IgA X24 (Glaudemans et al., 1990).

It seems clear from these studies that, despite both antibody and ligand diversity, the resulting antibody–hapten complexes can have remarkably similar geometries. Further studies will determine whether the orientation, and hence contact residues, of NPPC in the active site is the same in group II-A and group II-B antibodies. Such studies should also reveal whether NPPC and NPDBP have similar contacts in group II-B antibodies.

Acknowledgments

We thank M. Brown and Drs. Q. Chen and A. Buenafe for helpful discussions.

Registry No. PPC, 14093-45-9; NPPC, 21064-69-7; NPDBP, 120448-50-2.

References

Akutsu, H., & Kyogoku, Y. (1977) *Chem. Phys. Lipids 18*, 285.

Allinger, N. L. (1977) *J. Am. Chem. Soc. 99*, 8127.

Anglister, J., & Zilber, B. (1990) *Biochemistry 29*, 921.

Behling, R. W., Yamane, T., Navon, G., & Jelinski, L. W. (1988) *Proc. Natl. Acad. Sci. U.S.A. 85*, 6721.

Bruderer, U., Stenzel-Poore, M. P., Bächinger, H. P., Fellman, J. H., & Rittenberg, M. B. (1989) *Mol. Immunol. 26*, 63.

Chang, S. P., Brown, M., & Rittenberg, M. B. (1982) *J. Immunol. 128*, 702.
Clore, G. M., & Gronenborn, A. M. (1982) *J. Magn. Reson. 48*, 402.
Ernst, R. R., Bodenhausen, G., & Wokaun, A. (1987) *Principles of Nuclear Magnetic Resonance in One and Two Dimensions*, Clarendon, Oxford.
Glaudemans, C. P. J., Lerner, L., Daves, G. D., Jr., Kováč, P., Venable, R., & Bax, A. (1990) *Biochemistry 29*, 10906.
Keepers, J. W., & James, T. L. (1984) *J. Magn. Reson. 57*, 404.
Koide, S., Yokoyama, S., Matsuzawa, H., Miyazawa, T., & Ohta, T. (1989) *J. Biol. Chem. 264*, 8676.
Kumar, A., Ernst, R. R., & Wüthrich, K. (1980) *Biochem. Biophys. Res. Commun. 95*, 1.
Marion, D., & Wüthrich, K. (1983) *Biochem. Biophys. Res. Commun. 113*, 967.
Price, W. J. (1972) in *Laboratory Methods in Infrared Spectroscopy* (Miller, R. G. J., & Stace, B. C., Eds.) 2nd ed., p 115, Heydon and Sons, London.
Pullman, B., Berthod, H., & Gresh, N. (1975) *FEBS Lett. 53*, 199.
Richard, H., Dufourcq, J., & Lussan, C. (1974) *FEBS Lett. 45*, 136.
Satow, Y., Cohen, G. H., Padlan, E. A., & Davies, D. R. (1986) *J. Mol. Biol. 190*, 593.
Segal, D. M., Padlan, E. A., Cohen, G. H., Rudikoff, S., Potter, M., & Davies, D. R. (1974) *Proc. Natl. Acad. Sci. U.S.A. 71*, 4298.
Stenzel-Poore, M. P., & Rittenberg, M. B. (1989) *J. Immunol. 143*, 4123.
Zilber, B., Scherf, T., Levitt, M., & Anglister, J. (1990) *Biochemistry 29*, 10032.

Role of Glucose Carrier in Human Erythrocyte Water Permeability†

Mark L. Zeidel,*,‡ Ariela Albalak,‡ Eric Grossman,‡ and Anthony Carruthers§
Department of Medicine, West Roxbury Veterans Administration Medical Center, Brigham and Women's and Children's Hospitals, Harvard Medical School, 1400 V.F.W. Parkway, West Roxbury, Massachusetts 02132, and Department of Biochemistry and Molecular Biology and Program in Molecular Medicine, University of Massachusetts Medical School, 373 Plantation Street, Worcester, Massachusetts 01605

Received June 19, 1991; Revised Manuscript Received September 24, 1991

ABSTRACT: Although the transport properties of human erythrocyte water channels have been well characterized, the identity of the protein(s) mediating water flow remains unclear. Recent evidence that glucose carriers can conduct water raised the possibility that the glucose carrier, which is abundant in human erythrocytes, is the water channel. To test this possibility, water permeabilities and glucose fluxes were measured in large unilamellar vesicles (LUV) containing human erythrocyte lipid alone (lipid LUV), reconstituted purified human erythrocyte glucose carrier (Glut1 LUV), or reconstituted glucose carrier in the presence of other human erythrocyte ghost proteins (ghost LUV). In glucose and ghost LUV, glucose carriers were present at 25% of the density of native erythrocytes, were oriented randomly in the bilayer, and exhibited characteristic inhibition of glucose flux when exposed to cytochalasin B. Osmotic water permeability (P_f, in centimeters per second; $n = 4$) averaged 0.0012 ± 0.00033 in lipid LUV, 0.0032 ± 0.0015 in Glut1 LUV, and 0.006 ± 0.0014 in ghost LUV. Activation energies of water flow for the three preparations ranged between 10 and 13 kcal/mol; *p*-(chloromercuri)benzenesulfonate (pCMBS), an organic mercurial inhibitor of erythrocyte water channels, and cytochalasin B did not alter P_f. These results indicate that reconstitution of glucose carriers at high density increases water permeability but does not result in water channel activity. However, because the turnover number of reconstituted carriers is reduced from that of native carriers, experiments were also performed on erythrocyte ghosts with intact water channel function. In ghosts, P_f averaged 0.038 ± 0.013 ($n = 9$), while the activation energy for water flow averaged 3.0 ± 0.3 kcal/mol. Mercuric chloride reduced P_f by 93%, while pCMBS reduced it by 69%. Thus, ghosts retained water channel function. Preparation of ghosts in the presence of calcium led to markedly reduced glucose carrier activity without altering P_f. In addition, cytochalasin B did not reduce P_f. We conclude that the erythrocyte glucose carrier is not the water channel. The identity of the erythrocyte water channel remains elusive.

Although numerous transport studies have characterized the activity of a water channel in the plasma membrane of the human erythrocyte, the identity of this channel remains unclear (Macey, 1984; Finkelstein, 1986; Solomon, 1972). Estimates based on the high water permeability of erythrocyte plasma membranes suggest that each erythrocyte contains approximately 10^6 water channels (Finkelstein, 1986). These considerations suggest that proteins present in erythrocyte membranes in high density, such as the anion exchanger and the glucose carrier, are prime candidates to function as water channels (Macey, 1984; Finkelstein, 1986). Although the anion exchange protein is the most abundant membrane protein in the erythrocyte, several studies have dissociated

† Supported by NIH Grant RO-1 DK36081 awarded to A.C. and NIH Grant RO-1 DK43955 awarded to M.L.Z. M.L.Z. is the recipient of Research Career Development and Merit Review Awards from the Department of Veterans Affairs.
* Address correspondence to this author at Research Service, West Roxbury Veterans Administration Medical Center, 1400 V.F.W. Parkway, West Roxbury, MA 02132.
‡ West Roxbury Veterans Administration Medical Center, Brigham and Women's and Children's Hospitals, and Harvard Medical School.
§ University of Massachusetts Medical School.

0006-2960/92/0431-589$03.00/0